

Intermodal Coupling at the Junction Between Straight and Curved Waveguides

By C. P. BATES

(Manuscript received March 6, 1969)

This paper analyses the coupling of electromagnetic modes at the junction between straight and continuously curved rectangular waveguides. The method of solution is based on an integral equation formulation, applicable for sharp as well as gradual bends. Such quantities as the average power transmitted or reflected into each of the various modes propagating in the straight and curved waveguide sections are readily obtained.

The article presents the results of representative calculations for the two types of waveguide bends. These include graphs of the energy distribution in the transmitted and reflected modes as a function of dimensionless ratios for a sharp bend; the range of values considered allows immediate application of the results to standard C-band waveguides. The gradual bend example uses parameters encountered in the waveguide connections to an antenna in a typical microwave relay network.

I. INTRODUCTION

In a microwave system for guiding electromagnetic waves, often there are bends formed by connecting straight and continuously curved rectangular waveguides (see Fig. 1). Precise numerical computations and extensive analytical investigations of the angular propagation constants for the various electromagnetic modes in the curved section alone have been published by Cochran and Pecina.¹ The propagation constants and modal fields which may exist in the straight sections alone are trivial. To understand propagation of electromagnetic waves through these waveguide bends, therefore, requires a complete comprehension of the intermodal coupling that takes place at the various junctions and discontinuities. This paper investigates the coupling that occurs where straight and continuously curved rectangular waveguides join.

This type of structure has been studied to some extent by others.

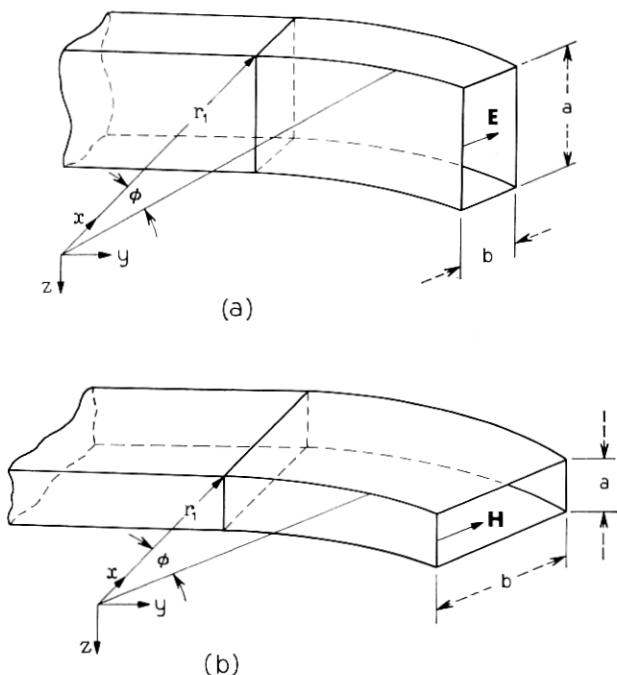


Fig. 1 — Waveguide bends formed by connecting straight and continuously curved rectangular waveguides. (a) E-plane bend. (b) H-plane bend.

There is an approach based on a matrix calculus formulation by Rice.² Using a perturbation method, Jouguet obtained expressions for the fields in the curved waveguide up to terms of second order, that is, to terms in $1/R^2$, where R denotes the radius of curvature of the axis of the curved guide.³ He uses these approximate expressions to determine the intermodal coupling that results at the junction between the straight and curved waveguides for a particular polarization of the field. In contrast with Jouguet's approach, the analysis we use permits the waveguide bends to be as sharp as desired, while still including the gradual bend within the permissible range of parameters.

Our approach involves the solution of a boundary value problem formulated in terms of the appropriate modal expansions for the fields in the straight and curved waveguides (see Section 2.1). The modal functions and propagation constants in these waveguide sections consist of certain combinations of trigonometric and Bessel functions and the zeros of such combinations. Evaluation of the appropriate quan-

tities for the curved waveguide is one of the more difficult aspects of this problem and necessitates not only numerical methods for determining zeros and asymptotic expansions but also computer algorithms for the accurate evaluation of Bessel functions. Such algorithms have been recently developed and programmed at Bell Telephone Laboratories.⁴

With the modal expansions in hand, one can formulate an integral equation for the aperture field at the junction between the straight and curved waveguides. This equation, as discussed in Section 2.2, may be solved numerically by the method of moments to within a reasonable accuracy (error criteria are discussed in Section 4.1). A solution for the fields in the waveguides can then be easily obtained, and such quantities as the power reflected or transmitted into various modes at the junction may be evaluated.

Section 4.2 gives examples of the intermodal power coupling for both sharp and gradual bends. Section 4.2.1 presents the results for the sharp bend example as a function of certain dimensionless ratios; the range of values considered allows direct application of the results to standard C-band waveguides. The results clearly demonstrate that significant intermodal power coupling takes place; they also establish the exaggeration which occurs in the reflected powers near the cutoff frequencies of the individual modes. Section 4.2.2 gives the results for the gradual bend example and shows that reflections are negligible and hence only the forward coupling has significant levels for the gradual bend considered.

II. FORMULATION AND SOLUTION OF THE BOUNDARY VALUE PROBLEM

2.1 *Fields in Straight and Continuously Curved Waveguides*

An arbitrary electromagnetic field, which may exist in either the straight or continuously curved waveguide, may be expressed as a sum of the longitudinal electric (*LE*) and longitudinal magnetic (*LM*) modes appropriate to that section (for explicit details on such modal representations in a continuously curved waveguide see Cochran and Pecina and for the straight waveguide see Harrington^{1, 5}). The *LE* modes have an electric field transverse to the *z*-direction which means this field component lies in the longitudinal plane, while the *LM* modes have their magnetic field similarly positioned.

The explicit form of the transverse components of the *LE* model expansion, suppressing an $\exp(j\omega t)$ time convention, is given below

(for a LE field and straight waveguide) :

$$\begin{aligned} {}^* \mathbf{E}^e &= \sum_{m,n} A_{mn}^{\pm} {}^* \mathbf{e}_{mn}^e \exp(\mp j\beta_{mn}y), \\ {}^* \mathbf{H}^e &= \pm \sum_{m,n} A_{mn}^{\pm} {}^* \mathbf{h}_{mn}^e \exp(\mp j\beta_{mn}y) \end{aligned} \quad (1)$$

with

$$\begin{aligned} {}^* \mathbf{e}_{mn}^e &= \varphi_m^e(x) \psi_n(z) \hat{x}, \\ {}^* \mathbf{h}_{mn}^e &= \frac{1}{j\beta_{mn}Z} \frac{d}{dx} \varphi_m^e(x) \frac{d}{dz} \psi_n(z) \hat{x} + \frac{h_n^2}{j\beta_{mn}Z} \varphi_m^e(x) \psi_n(z) \hat{z}, \\ \varphi_m^e(s) &= (\epsilon_m/b)^{\frac{1}{2}} \cos[m\pi/b(r_2 - x)], \\ & \quad m = 0, 1, 2, \dots, \quad \epsilon_0 = 1, \quad \epsilon_m = 2, \quad m \geq 1, \\ \psi_n(z) &= (2/a)^{\frac{1}{2}} \sin(n\pi z/a), \quad n = 1, 2, \dots, \\ \beta_{mn} &= [h_n^2 - (m\pi/b)^2]^{\frac{1}{2}} = -j[(m\pi/b)^2 - h_n^2]^{\frac{1}{2}}, \quad m = 0, 1, 2, \dots, \\ h_n &= [k^2 - (n\pi/a)^2]^{\frac{1}{2}}, \quad n = 1, 2, \dots, \end{aligned}$$

and

$$k = \omega/c, \quad Z = j\omega\mu, \quad r_2 = r_1 + b.$$

Here ${}^* \mathbf{E}^e$ is the transverse electric field intensity, ${}^* \mathbf{H}^e$ the transverse magnetic field intensity, ω the angular frequency, k the wave number, μ the permeability, and c the phase velocity of the medium filling the guide. The vector components which make up the field are given by the lower case letters. The A_{mn}^{\pm} are the unknown expansion coefficients of the individual LE modes in the straight guide with the (\pm) indicating waves traveling either in the positive or negative y -direction (towards or away from the junction in the straight section of Fig. 1a). The propagation constant of a particular mode is β_{mn} , and it is either real or purely imaginary (providing the guide is filled with a lossless medium) thus indicative of either a traveling or evanescent mode.

In the curved waveguide, using polar coordinates (ρ, φ, z) , one has (for the LE field and curved guide) :

$$\begin{aligned} {}^* \mathbf{E}^e &= \sum_{m,n} C_{mn}^{\pm} {}^* \mathbf{e}_{mn}^e \exp(\mp j\nu_{mn}\varphi), \\ {}^* \mathbf{H}^e &= \pm \sum_{m,n} C_{mn}^{\pm} {}^* \mathbf{h}_{mn}^e \exp(\mp j\nu_{mn}\varphi) \end{aligned} \quad (2)$$

with

$${}^* \mathbf{e}_{mn}^e = \frac{1}{\rho} \varphi_{mn}^e(h_n, \rho) \psi_n(z) \hat{\rho},$$

$$\mathbf{h}_{mn}^e = \frac{1}{j\nu_{mn}Z} \frac{d}{d\rho} \varphi_{mn}^c(h_n\rho) \frac{d}{dz} \psi_n(z) \hat{\rho} + \frac{h_n^2}{j\nu_{mn}Z} \varphi_{mn}^c(h_n\rho) \psi_n(z) \hat{z},$$

$$\varphi_{mn}^c(h_n\rho) = C_{\nu_{mn}}(h_n\rho) / \| C_{\nu_{mn}}(h_n\rho) \|,$$

$$C_{\nu_{mn}}(h_n\rho) = J'_{\nu_{mn}}(h_n r_2) Y_{\nu_{mn}}(h_n\rho) - Y'_{\nu_{mn}}(h_n r_2) J_{\nu_{mn}}(h_n\rho),$$

and

$$\| C_{\nu_{mn}}(h_n\rho) \| = \left(\int_{r_1}^{r_2} C_{\nu}^2/\rho \, d\rho \right)^{\frac{1}{2}}.$$

In these expressions $J_\nu(x)$ and $Y_\nu(x)$ are the Bessel functions of the first and second kind respectively; the prime indicates differentiation with respect to the argument. The permissible propagation numbers ν_{mn} , in this case, are given by the implicit solutions of

$$\frac{d}{d\rho} C_{\nu_{mn}}(h_n\rho) \big|_{\rho=r_1} = 0, \quad m = 0, 1, 2, \dots,$$

and again they are either real or purely imaginary providing the guide is filled with a lossless medium.⁶ Section III discusses the modal function, C_ν , in more detail. The C_{mn}^\pm are the expansion coefficients of the individual modes with the (\pm) again designating the direction of mode travel.

In equations (1) and (2) the superscript e indicates that the particular vector is an LE component and the superscript s or c indicates that the vector or function is associated with the straight or curved sections. The subscripts m and n are the modal indices. In Section IV, where results are also given for an LM polarization, a superscript m designates such fields.

One may easily verify that these transverse LE field components, along with their longitudinal counterparts, satisfy Maxwell's equations in the appropriate regions and that the required boundary conditions, namely, zero tangential electric field and zero normal magnetic field on the waveguide walls, are met. Such representations are complete in that any arbitrary fields in the straight and curved waveguides which have their electric components confined to the longitudinal plane can be expanded in the form of equation (1) or (2), respectively.

Appropriate expressions may also be written for the transverse components of the LM modal expansions. They would also be complete in the sense that any arbitrary fields in the straight and curved waveguides which have their magnetic components confined to the longitudinal plane could be expanded in such a representation.

It can be shown, for the geometry indicated in Fig. 1, that an LE

source in either the straight or curved waveguide excites only an LE field, and conversely an LM source excites only an LM field. Hence a waveguide bend excited by an LE mode is usually referred to as an E-plane bend, in keeping with the fact that the LE source sets up only an LE field for which the electric field is confined to the longitudinal plane, that is, the plane of the bend. Figure 1a shows the typical waveguide geometry for an E-plane bend. Analogously, an H-plane bend is one for which the magnetic field is confined to the plane of the bend; this occurs when the source and hence the resulting fields are LM . Figure 1b shows typical geometry for this case.

Notice that the transverse vector components can be shown to satisfy

$$\iint^* \mathbf{e}_{mn}^c \cdot \mathbf{e}_{rs}^c dA = \delta_{mr} \delta_{ns}^\dagger, \quad \iint^c \mathbf{e}_{mn}^c \cdot \mathbf{e}_{rs}^c \rho dA = \delta_{mr} \delta_{ns}. \quad (3)$$

In equation (3) the integration is taken over the cross-sectional area of the appropriate waveguide interior. Such orthogonalities are a consequence of the differential equations and the boundary conditions satisfied by the scalar parts of the transverse vector components.

2.2 Integral Equation Formulation and Solution

As discussed in Section 2.1, the fields in the guides need only be expanded in a representation consistent with the given source. In the sequel, the unknown coefficients of the modal expansions are determined through an integral equation approach.

If there are LE modes incident on the junction in Fig. 1a in both the straight and curved guides, the continuity in the transverse electric and magnetic fields at the junction between the guides requires

$$S_{rs}^s \mathbf{e}_{rs}^s + \sum_{m,n} A_{mn}^- \mathbf{e}_{mn}^s = \sum_{m,n} C_{mn}^+ \mathbf{e}_{mn}^c + S_{rs}^c \mathbf{e}_{rs}^c \quad (4)$$

and

$$S_{rs}^s \mathbf{h}_{rs}^s - \sum_{m,n} A_{mn}^- \mathbf{h}_{mn}^s = \sum_{m,n} C_{mn}^+ \mathbf{h}_{mn}^c - S_{rs}^c \mathbf{h}_{rs}^c. \quad (5)$$

Here the source coefficients have been designated, for emphasis, by S_{rs}^s and S_{rs}^c , for the straight and curved sections, respectively; they are assumed specified. The unknowns are the modal expansion coefficients A_{mn}^- and C_{mn}^+ .

Each side of equation (4) is actually an expansion of the unknown aperture electric field $\mathbf{E}_a(x, z)$. Referring to the orthogonal properties of

† Kronecker delta.

the transverse vector components in Section 2.1, it follows that

$$S_{r,s}^+ \delta_{mr} \delta_{ns} + A_{mn}^- = \iint_{S_A} \mathbf{E}_a \cdot {}^s \mathbf{e}_{mn}^+ dA \quad (6)$$

and

$$C_{mn}^+ + S_{r,s}^c \delta_{mr} \delta_{ns} = \iint_{S_A} \mathbf{E}_a \cdot {}^c \mathbf{e}_{mn}^+ \rho dA \quad (7)$$

for $m = 0, 1, \dots$ and $n = 1, 2, \dots$ with the integration being performed over the aperture area.[†] Rearranging equation (5) and substituting the relationships (6) and (7) for the expansion coefficients results in:

$$2S_{r,s}^+ {}^s \mathbf{h}_{r,s}^+ + 2S_{r,s}^c {}^c \mathbf{h}_{r,s}^+ = \iint_{S_A} \mathbf{E}_a(x', z') \cdot \bar{\mathbf{G}}(x, z; x', z') dA', \quad (8)$$

where the dyadic kernel is given by

$$\bar{\mathbf{G}}(x, z; x', z') = \sum_{m,n} [{}^s \mathbf{e}_{mn}^+(x', z') {}^s \mathbf{h}_{mn}^+(x, z) + {}^c \mathbf{e}_{mn}^+(x', z') {}^c \mathbf{h}_{mn}^+(x, z)]. \quad (9)$$

Notice that equation (8) is precisely in the form of a vector Fredholm integral equation of the first kind for the unknown aperture electric field.

A solution of this integral equation by the method of moments would proceed as follows.⁷ Expanding the aperture electric field in terms of the modes of the straight waveguide gives

$$\mathbf{E}_a(x, z) = \sum_{m,n} a_{mn} {}^s \mathbf{e}_{mn}^+ \quad (10)$$

Substituting into equation (8) and interchanging summation and integration then requires

$$2S_{r,s}^+ {}^s \mathbf{h}_{r,s}^+ + 2S_{r,s}^c {}^c \mathbf{h}_{r,s}^+ = \sum_{m,n} a_{mn} ({}^s \mathbf{h}_{mn}^+ + \sum_p b_{mpn} {}^c \mathbf{h}_{pn}^+), \quad (11)$$

with b_{mpn} defined by

$$b_{mpn} = \int_{r_1}^{r_2} \varphi_m^s(x) \varphi_{pn}^c(h_n x) dx. \quad (12)$$

Taking the inner product of equation (11) with ${}^s \mathbf{h}_{j\alpha}^+$ finally leads, after some algebra, to

[†] The indices m and n of the modes are chosen such that in the limit of $r_1 \rightarrow \infty$ the mode in the curved guide with index numbers m and n is asymptotic to the mode in the straight guide with index numbers m and n .

$$\frac{2S_{rs}^a}{\beta_{rs}} \delta_{jr} \delta_{qs} + \frac{2S_{rs}^c}{\nu_{rs}} b_{irs} \delta_{qs} = \sum_m a_{mq} \left(\frac{\delta_{jm}}{\beta_{mq}} + \sum_p \frac{b_{mpq} b_{ipq}}{\nu_{pq}} \right),$$

$$j = 0, 1, 2, \dots, \quad q = 1, 2, \dots \quad (13)$$

as the infinite set of algebraic equations to be solved for a_{mq} , the expansion coefficients of the aperture electric field.

As a first observation, we note from equation (13) that $a_{mq} \equiv 0$ if $q \neq s$, and hence the aperture field is actually given by

$$\mathbf{E}_a(x, z) = \sum_m a_{ms} \mathbf{e}_{ms}^*(x, z), \quad (14)$$

that is, the z -variation of the excited modes is the same as the z -variation of the source mode. At this point, therefore, the second subscript may be dropped without loss of generality by merely realizing it is the same as the second subscript of the exciting modes.

Equations (13) form an infinite set of equations for the infinite number of unknown expansion coefficients of the aperture field. A truncation is now made in order to solve for a_m by standard matrix methods, including sufficient terms in the field expansions in order to ensure reasonable accuracy (see Section 4.1).[†]

2.3 Reflected and Transmitted Modes

Let us assume here that the expansion coefficients for the aperture field have been obtained by solving equation (13). A relationship between the coefficients of the modes in the straight guide and the aperture field was given by equation (6). Substituting the expansion of the aperture field, equation (14), into this equation gives an expression for the coefficients of the modes in the straight guide as

$$A_m^- = a_m - \delta_{mr} S_r^a, \quad m = 0, 1, 2, \dots \quad (15)$$

Likewise equation (7) yields, for the coefficients of the modes excited in the curved waveguide,

$$C_m^+ = \sum_q a_q b_{qm} - \delta_{mr} S_r^c, \quad m = 0, 1, 2, \dots \quad (16)$$

These relations are deceptively simple in that much of the complex interplay between incident, reflected, and transmitted modes is hidden in the "assumed known" coefficients a_m and a_q .

The average power carried by the incident r th mode in the straight

[†] The solution of equation (13) also requires knowledge of the b_{mp} defined by equation (12). Their determination is at the crux of this method and their evaluation will be discussed in Section 3.

and curved guide may be determined:

$$PI_r^* = - \iint {}^*E_x^c {}^*H_z^{c*} ds = \frac{h^2}{j\beta_r Z^*} |S_r^*|^2 \quad (17)$$

and

$$PI_r^c = \iint {}^cE_x^c {}^cH_z^{c*} ds = \frac{h^2}{j\nu_r Z^*} |S_r^c|^2. \quad (18)$$

Here we assume that the incident r th mode is a propagating mode with real β_r and ν_r , and that (*) designates the complex conjugate of a quantity.

The average power coupled into the m th mode from the incident r th mode may be evaluated in a similar manner yielding for the straight guide

$$PC_{mr}^* = \frac{h^2}{j\beta_m Z^*} |A_m^-|^2 \quad (19)$$

and for the curved guide

$$PC_{mr}^c = \frac{h^2}{j\nu_m Z^*} |C_m^+|^2. \quad (20)$$

The index m in equations (19) and (20) is anyone such that β_m or ν_m is real; that is, the m th mode must be a propagating one which carries energy away from the junction. There are, of course, only a finite number of such propagating modes for a particular operating frequency (see Cochran and Pecina¹).

Equations (19) and (20) thus determine the power coupling, that is, the power excited in the m th propagating mode either transmitted or reflected when the r th mode is incident in either the straight or curved sections. Naturally, these quantities become of dominant importance as one moves away from the junction and the evanescent modal contributions die out. Section 4.2 gives some examples of the power coupling for both sharp and gradual bends.

A similar analysis can be performed for an LM excitation. Section IV presents the numerical results for this case.

III. PROPAGATION CONSTANTS AND MODAL FUNCTIONS

The modal functions for the continuously curved waveguide are de-

† At this stage we assume that the waveguides are filled with a lossless dielectric; hence, the total power is the sum of the power in each individual mode.

defined in terms of Bessel functions of the first and second kind in Section 2.1. Obviously they are solutions of Bessel's differential equation, which we write in the form

$$\frac{1}{\rho} \frac{d}{d\rho} \left(\rho \frac{d}{d\rho} C_{\nu_{mn}} \right) + \left(h_n^2 - \frac{\nu_{mn}^2}{\rho^2} \right) C_{\nu_{mn}} = 0; \quad (21)$$

moreover, for LE excitation, they are such that

$$\frac{d}{d\rho} C_{\nu_{mn}}(h_n \rho) \Big|_{\rho=r_1} = 0. \quad (22)$$

The boundary condition at $\rho = r_2$ is automatically satisfied by the particular choice of the cross-product Bessel functions in Section 2.1, whereas the boundary condition at $\rho = r_1$ determines the admissible angular propagation constants ν_{mn} .

The real angular propagation constants result in propagating modes and hence are the most important in this analysis. These are obtained for the sharp bend by a program of precise calculations of the real ν -solutions of the transcendental equation (22). The Bessel functions appearing in equation (22) were approximated with six-figure accuracy by the use of algorithms recently developed and programmed for a digital computer as discussed in Ref. 1.

There are other methods to determine the propagation constants of gradual bends. For instance, a large parameter expansion of the differential equation (21) can be made; that is, the modal functions and propagation constants may both be expanded in negative powers of r_2 . The unknown coefficients of each series can then be determined by imposing the boundary conditions at $\rho = r_1$ and r_2 . This approach has been used by Kislyuk, as well as others; Ref. 8 gives these results. Four terms in the expansion are all that are available, because higher order terms are extremely tedious to determine.

A comparison of the real values of ν evaluated from Kislyuk's results with the precise ν -zeros of equation (22) shows five digit agreement for gradual bends ($r_1/b > 12$). In the final program, we chose to calculate all angular propagation constants by Kislyuk's equation for large (r_1/b), that is, 12 or greater.

In the sharp bend case the imaginary propagation constants cannot be obtained precisely, because there are no computer algorithms for the evaluation of Bessel functions for this range (imaginary orders). So other techniques must be used.

When the propagation constants lie on the negative imaginary axis,

that is, $\nu = -i\mu$ and μ is not close to zero, asymptotic expansions for the modal functions can be obtained. One approach is to approximate the Bessel functions in C_ν (the derivative with respect to $h_n r_2$ is not performed as yet) by the first term of the asymptotic series developed by Olver.⁹ This yields an expression in terms of the familiar Airy functions Ai and Bi . When the Airy functions are approximated by the leading terms of their phase-amplitude expansions (see Abromowitz and Stegun¹⁰) and the derivative with respect to $h_n r_2$ is taken, the approximation of C_ν becomes

$$C_\nu \approx \frac{-2}{\pi\mu[(1 + \zeta^2\eta^2)(1 + \eta^2)]^{\frac{1}{2}}} \left\{ (1 + \eta^2)^{\frac{1}{2}}/\eta \cos [\mu(\omega(\eta) - \omega(\zeta\eta))] + \frac{\eta}{2\mu(1 + \eta^2)} \sin [\mu(\omega(\eta) - \omega(\zeta\eta))] \right\}, \quad (23)$$

where

$$\eta = \frac{hr_2}{\mu}, \quad \zeta = \frac{r}{r_2},$$

and

$$\omega(\eta) = \ln \left[\frac{1 + (1 + \eta^2)^{\frac{1}{2}}}{\eta} \right] - (1 + \eta^2)^{\frac{1}{2}}.$$

The imaginary propagation constants for the sharp bend are now determined by numerically finding the μ -zeros of the asymptotic expressions, equation (23).

The evaluations of the inner products, equation (12), required in Section 2.2 are performed numerically. When the propagation constants are real, we again use the computer algorithms for the evaluation of the Bessel functions for both the sharp and gradual bends. The latter evaluation was required because the evaluation of the modal functions by means of a large parameter series expansion as determined by Kislyuk's approach (really only three terms available) does not exhibit very good agreement with the precise evaluation of the modal function even in a region where the agreement between the two methods of determining the propagation constant is very good. When the propagation constants are imaginary the modal functions for the curved waveguide are evaluated by means of the approximate expression, equation (3), for both the sharp and gradual bends.

A similar analysis may be made for an *LM* polarization; Section IV presents the results of appropriate numerical calculations, as well as,

comments concerning the verification of the numerical solution and some representative examples.

IV. ERROR CRITERIA AND REPRESENTATIVE EXAMPLES

4.1 Error Criteria

As discussed in Section 2.2, the solution of the integral equation for the aperture field reduces to an infinite set of algebraic equations for its expansion coefficients. We make a truncation so that standard matrix techniques may be used to solve for these unknown coefficients. Sufficient terms must be included to obtain reasonable accuracy; including more terms than necessary wastes computing time.

One can verify that a particular truncation is adequate by determining how well the field solutions satisfy the continuity requirement at the aperture. The conservation of energy, which requires that the average power in all the propagating modes traveling away from the junction between the guides be equal to the average power in the propagating modes incident on the junction, is always satisfied (within roundoff error) by the solution obtained (that is, regardless of the number of modes used); therefore it cannot be used as an accuracy check. This redundancy in the conservation of power, which may be established by an analysis suggested by Amitay and Galindo,¹¹ is a consequence of the method of moments approach which has been used to solve the integral equation.

When the incident field is an LE mode, the aperture electric field is determined. From this field one can derive the modal coefficients and hence the magnetic fields in the straight and curved guides. These derived magnetic fields should be continuous at the aperture; therefore, a mean square error (MSE—refer to its application by Cole and others¹²), normalized with respect to the incident field, can be defined as

$$\text{MSE} = \frac{\iint (\mathbf{H}^e - \mathbf{H}^i) \cdot (\mathbf{H}^e - \mathbf{H}^i)^* ds}{\iint (\mathbf{H}_i + \mathbf{H}_e) \cdot (\mathbf{H}_i + \mathbf{H}_e)^* ds}$$

The subscript i designates the incident exciting field; the terms in the numerator constitute the total fields, all evaluated at the junction between the guides. This mean square error is a meaningful measure of how well continuity in the aperture field is approached, and is, of course, a function of the number of modes used in expanding the fields.

It was found, in the examples of Section 4.2, that the mean square error could be maintained smaller than 10^{-5} . This corresponds to three to four digit agreement between the samples of the transverse components of the magnetic fields on both sides of the aperture. A similar mean square error may be defined for the *LM* case with corresponding error levels.

4.2 Representative Examples

Some of the following representative examples correspond to very sharp bends ($r_1/b \approx 1$); the others correspond to very gradual bends ($r_1/b \gg 1$).

4.2.1 Sharp Bends

Figures 2 through 5 and Table I give the results for the sharp bends. We give the power transmitted into the modes of the curved guide and reflected into the modes of the straight guide for an incident mode in the straight guide in terms of the dimensionless ratios b/λ , r_1/b , and a/b . Any structure with these ratio numbers has a coupling characteristic as displayed.

The incident modes used in Figs. 2 and 3 are from the set of $LM_{m_0}^*$ modes in the straight guide which have an electric field given by

$$\mathbf{E}_{m_0}^* = \frac{-B_{m_0}^+ h_0^2}{j\beta_{m_0} Y} (2/b)^{\frac{1}{2}} \sin [m\pi/b(r_2 - x)] \exp(-j\beta_{m_0} y) \hat{z}.$$

That is, the incident fields are the familiar TE_{m_0} modes of a uniform rectangular guide. The curved guides used here are referred to as H-plane bends since the magnetic field lies in the plane of the bend (see Section 2.1). In Figs. 4 and 5 the incident modes are from the $LE_{m_1}^*$ mode set in the straight guide. The curved guides there are referred to as E-plane bends since the electric field lies in the plane of the bend. The $LE_{0_1}^*$ mode incident corresponds to the familiar TE_{0_1} mode with an electric field given by

$$\mathbf{E}_{0_1}^* = A_{0_1}^+ (2/ab)^{\frac{1}{2}} \sin(\pi z/a) \exp(-j\beta_{0_1} y) \hat{x}$$

whereas the $LE_{1_1}^*$ mode incident is a combination of the TE_{1_1} and TM_{1_1} modes in a uniform rectangular guide. The coefficients $B_{m_0}^+$ and $A_{m_1}^+$ of the incident modes are chosen so that the incident power is unity.

The sharp bend results may be used, for example, to depict the operation of the standard C-band guide 0.872 by 1.872 inch for a frequency range from 3 to 18 GHz for the *LM* excitation and from 3 to 20 GHz for the *LE* excitation. For convenience we have superimposed

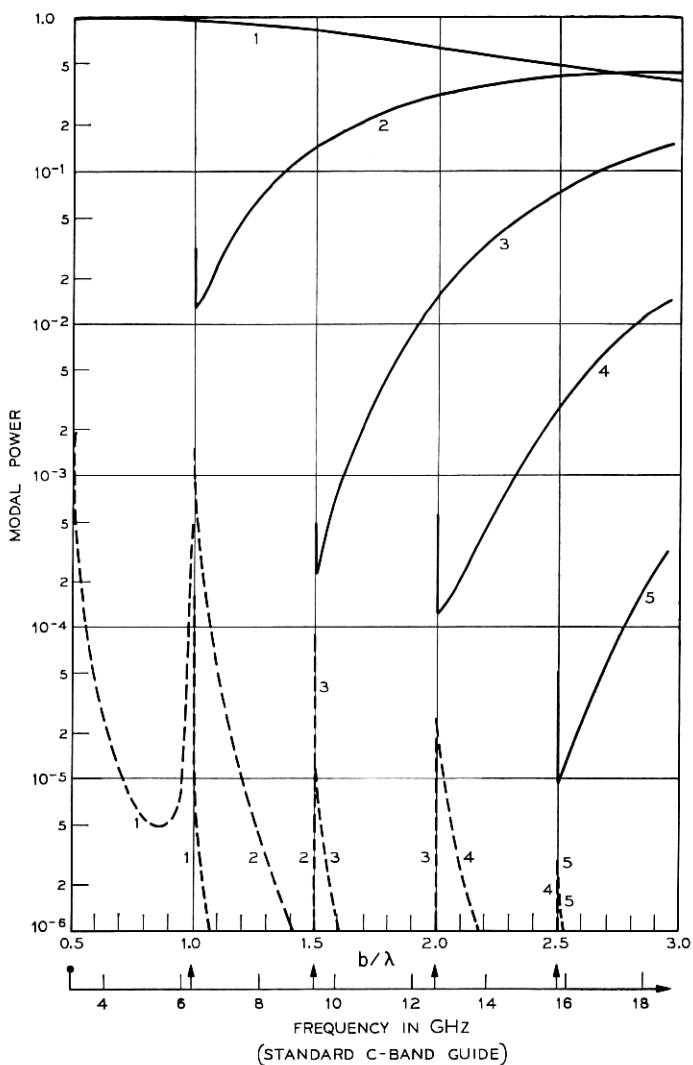


Fig. 2 — Intermodal coupling at H-plane bend — sharp bend case. (Incident mode = LM_{10}^s ; incident power = 1.0; $r_1/b = 1.068$; $a/b = 0.466$.) Solid line is for a curved guide; dashed line is for a straight guide.

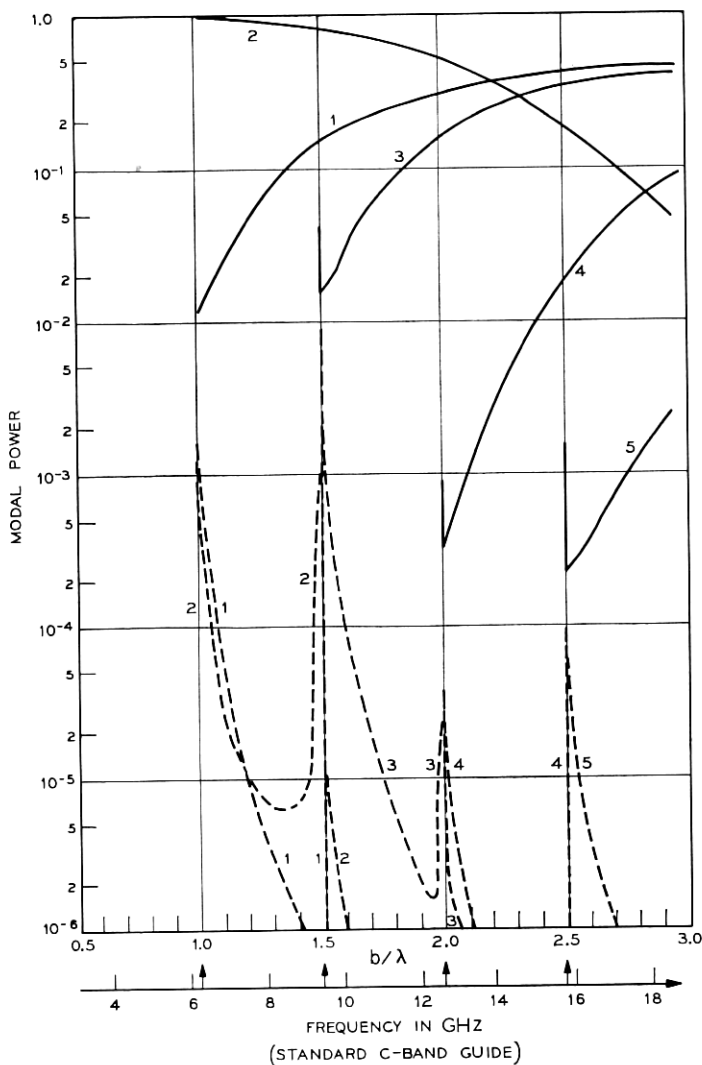


Fig. 3 — Intermodal coupling at H-plane bend — sharp bend case. (Incident mode = LM_{20}^* ; incident power = 1.0; $r_1/b = 1.068$; $a/b = 0.466$.) Solid line is for a curved guide; dashed line is for a straight guide.

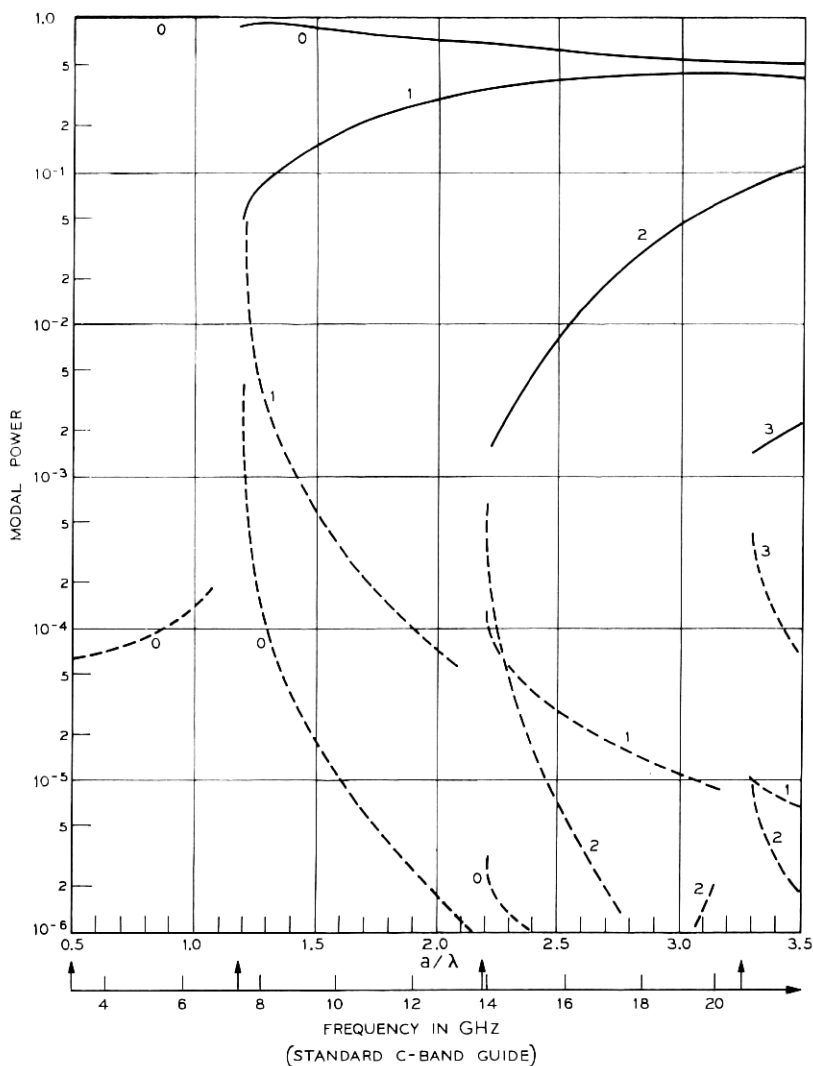


Fig. 4 — Intermodal coupling at E-plane bend — sharp bend case. (Incident mode = LE_{01}^* ; incident power = 1.0; $r_1/b = 1.148$; $a/b = 2.15$.) Solid line is for a curved guide; dashed line is for a straight guide.

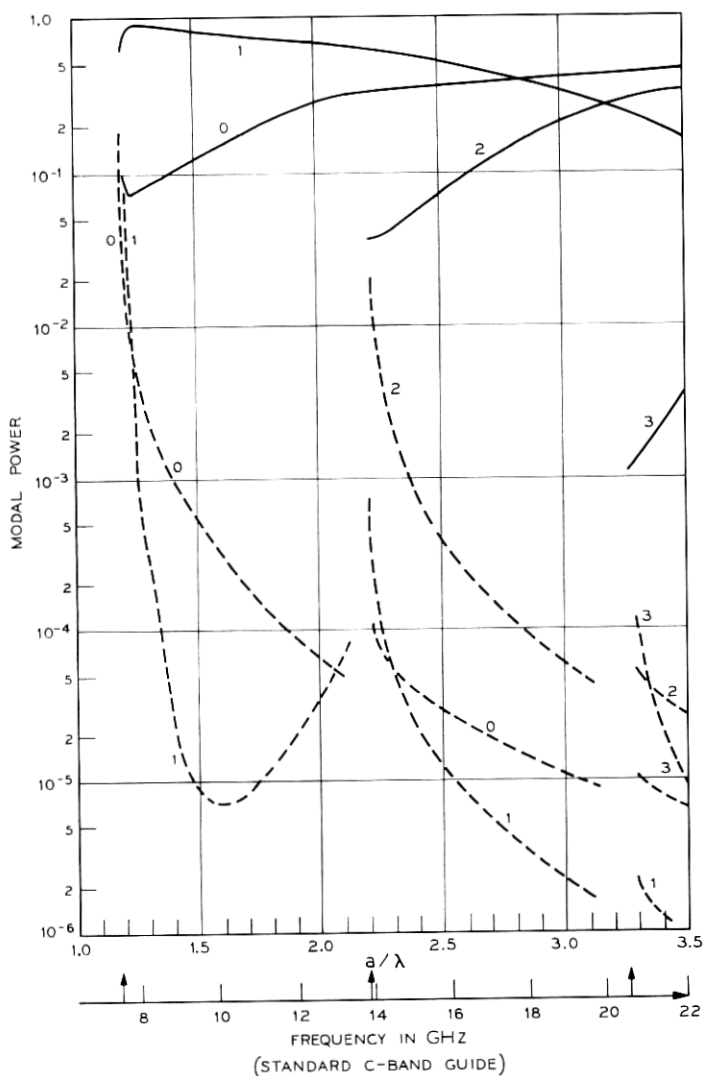


Fig. 5 — Intermodal coupling at E-plane bend — sharp bend case. (Incident mode = LE_{11}^s ; incident power = 1.0; $r_1/b = 1.148$; $a/b = 2.15$.) Solid line is for a curved guide; dashed line is for a straight guide.

TABLE I—INTERMODAL COUPLING FOR LONGITUDINAL ELECTRIC AND LONGITUDINAL MAGNETIC FIELDS FOR A SQUARE GUIDE WITH $r_1/b = 1.068$

b/λ	Incident Mode Power	Reflected Mode Power	Transmitted Mode Power
1.19	$LM_{10}^s = 1.0$	$LM_{10}^s \approx 10^{-7}$	$LM_{10}^c = 0.952174$
		$LM_{20}^s = 0.000012$	$LM_{20}^c = 0.047815$
	$LE_{01}^s = 1.0$	$LE_{01}^s = 0.000001$	$LE_{01}^c = 0.618860$
		$LE_{11}^s = 0.000046$	$LE_{11}^c = 0.376074$
1.79	$LM_{10}^s = 1.0$	$LE_{21}^s = 0.000022$	$LE_{21}^c = 0.004997$
		$LM_{10}^s = 10^{-9}$	$LM_{10}^c = 0.736720$
		$LM_{20}^s = 0.000001$	$LM_{20}^c = 0.258699$
		$LM_{30}^s \approx 10^{-7}$	$LM_{30}^c = 0.004581$
	$LE_{01}^s = 1.0$	$LE_{01}^s \approx 10^{-7}$	$LE_{01}^c = 0.456751$
		$LE_{11}^s = 0.000005$	$LE_{11}^c = 0.384346$
		$LE_{21}^s = 0.000001$	$LE_{21}^c = 0.153564$
		$LE_{31}^s = 0.000027$	$LE_{31}^c = 0.005306$

another coordinate scale on Figs. 2 through 5 demonstrating the frequency of operation if the guide has these dimensions. The vertical arrows on this frequency scale indicate the cutoff frequencies of the modes in the straight guide. As these examples show, the frequency band covered corresponds to a situation where up to 5 modes can propagate. The overmoded operation demonstrates the possible coupling between modes. Also notice that for the H-plane bend (Figs. 2 and 3), b is greater than a and for the E-plane bend (Figs. 4 and 5) b is less than a .

The strong coupling between the modes for sharp bends is clearly demonstrated for H-plane bends in Figs. 2 and 3. In Fig. 2 we see that the LM_{10}^s mode incident in the straight guide can actually couple more energy into the LM_{20}^c than into the LM_{10}^c mode of the curved guide when b/λ is greater than 2.7. Conversely the LM_{20}^s mode incident in the straight guide can couple more energy into the LM_{10}^c , LM_{30}^c , and LM_{40}^c modes than into the LM_{20}^c mode of the curved guide for the appropriate b/λ , as Fig. 3 shows.

For an LM excitation it is possible to have a mode propagating in the curved waveguide while still cut off in the straight waveguide. This leads to a value of coupling into the curved guide mode which drops sharply as the corresponding mode begins to propagate in the straight guide but then increases with increasing frequency. Figures 2 and 3 show this at $b/\lambda = 1.0, 1.5, 2.0,$ and 2.5 . The reflections are also exaggerated at the cutoff frequencies of the modes in the straight guide. In

contrast, the cutoff frequencies of the LE modes in the curved guide are greater than or equal to those in the straight guide. This leads to the possibility of having a mode propagating in the straight guide while still cut off in the curved guide. Sharp jumps in reflections and transmissions are thus also expected at such cutoff frequencies for this situation; unfortunately, we are not able to examine them in detail. Recall that the procedure outlined in Section III allows us only to find the imaginary propagation constants in the curved waveguide if they are not too small. Unfortunately the case just described violates this restriction since the pertinent propagation constants in the curved waveguide are imaginary with a magnitude infinitesimally close to zero.

In Figs. 4 and 5 one can see that the power coupling at an E-plane bend is also very strong. The reflections for this case are more pronounced over a wider frequency band than in the H-plane case. Again there are exaggerated reflections at the cutoff frequencies of the modes. Notice that with both LE and LM polarizations, the forward coupling is greatest into the modes adjacent to the one corresponding to the incident mode.

It is valuable to compare the coupling for an E-plane bend with that of a H-plane bend for equivalent problems. To this end, consider a square guide with the ratio r_1/b set at 1.068 for each polarization and the frequency of operation set at the same value for both cases. Table I gives the coupling for this situation. (Notice that the number of LE modes propagating is one more than the number of LM modes propagating at the frequencies used.) From the results one sees that much less energy is forward coupled into the mode corresponding to the incident one when the fields are LE and that the total reflected energy is greater in the LE case. This is not unexpected if one examines the discontinuity in the geometry encountered by the electric field intensity for both cases.

4.2.2 Gradual Bends

For a very gradual bend situation we chose square waveguides with $r_1/b = 250$. This very gradual bend simulates the curvatures encountered in the waveguide connection between receiver and antenna of the Bell System TD-2 microwave relay system (one must realize though that waveguides with circular cross sections are used there). Tables II and III give some pertinent results. Again a frequency scale is superimposed, this time corresponding to a 2.4 inch guide. This value was picked so that the fundamental mode in the straight guide with a square

cross section would have the same propagation constant as the fundamental mode of a straight guide with a circular cross section, 2.812 inches in diameter. This we felt, permits us to stimulate, at least qualitatively, the situation encountered with circular cross section guides in the TD-2 system.

The coupling in the reverse direction (reflected power) was at least 60 dB down for both LE and LM fields regardless of which mode was incident; hence these tables do not give them. The H-plane bend (Table II) forward couples power (≈ 40 dB down) into modes adjacent to the one corresponding to the incident mode only at the higher frequencies. The E-plane bend (Table III) exhibits much larger forward coupled power into such modes (≈ 30 dB down) at these same higher frequencies. The levels of the undesired forward coupling at the lower frequencies is much less (≈ 50 dB down). The results suggest that with such gradual bends reverse coupling is totally insignificant and only forward coupling can have a meaningful effect.

All the results discussed in Section 4.2 have been based on the excitation from the straight guide side of the junction. The results for excitation from the curved guide side are of the same form, and hence, have not been given for the sake of brevity. However, forward coupling into the straight guide from the curved guide may be deduced from the data already presented by realizing that the power forward coupled into mode m of the straight guide from mode n in the curved

TABLE II—INTERMODAL COUPLING RESULTING FROM A LONGITUDINAL MAGNETIC MODE INCIDENT IN STRAIGHT GUIDE WITH $r_1/b = 250$

b/λ	f ($b = 2.4$ inches) GHz	Incident Mode	Excited Mode	Excited Mode Power Level (dB)
0.813	4	LM_{10}^s	LM_{10}^c	0.00
1.22	6	LM_{10}^s	LM_{10}^c	0.00
			LM_{20}^c	-55.84
		LM_{20}^s	LM_{10}^c	-55.84
			LM_{20}^c	0.00
2.24	11	LM_{10}^s	LM_{10}^c	0.00
			LM_{20}^c	-41.54
			LM_{30}^c	< -60
			LM_{40}^c	< -60
		LM_{20}^s	LM_{10}^c	-41.54
			LM_{20}^c	0.00
			LM_{30}^c	-47.59
			LM_{40}^c	< -60

TABLE III—INTERMODAL COUPLING RESULTING FROM A LONGITUDINAL ELECTRIC MODE INCIDENT IN STRAIGHT GUIDE WITH $r_1/b = 250$

b/λ	f ($b = 2.4$ inches) GHz	Incident Mode	Excited Mode	Excited Mode Power Level (dB)
0.813	4	LE_{01}^s	LE_{01}^c	0.00
			LE_{11}^c	-50.06
1.22	6	LE_{11}^s	LE_{01}^c	-50.06
			LE_{11}^c	0.00
		LE_{01}^s	LE_{01}^c	0.00
			LE_{11}^c	-39.39
2.24	11	LE_{11}^s	LE_{21}^c	< -60
			LE_{01}^c	-39.39
			LE_{11}^c	0.00
			LE_{21}^c	-55.46
		LE_{01}^s	LE_{01}^c	-0.01
			LE_{11}^c	-27.38
			LE_{21}^c	< -60
			LE_{31}^c	< -60
			LE_{41}^c	< -60
			LE_{01}^c	-27.38
LE_{11}^s	LE_{11}^c	-0.01		
	LE_{21}^c	-39.88		
	LE_{31}^c	< -60		
	LE_{41}^c	< -60		

guide is the same as the power forward coupled into mode n of the curved guide from mode m in the straight guide (reciprocity).[†]

V. CONCLUSION

This paper has investigated the coupling of electromagnetic waves between straight and curved rectangular waveguides. Numerical results have been obtained by using a numerical method which leads to solutions applicable for sharp as well as gradual bends. Two representative examples have been given. One was a sharp bend and could be used to depict the coupling that takes place, say, in standard C-band guides. The other was a very gradual bend; this was used to obtain some insight into the coupling that occurs in the waveguide connections between the receiver and antenna in typical microwave networks.

The coupling discussed has been confined to a one junction struc-

[†] This modal reciprocity, although surprising at first glance, is a direct consequence of Maxwell's equations, the lossless character of the guides, and the orthogonalities between the modes as discussed in Section 2.1.

ture, that is, a straight to a curved guide or a curved to a straight guide. In any practical system, however, at least two junctions generally occur, that is, one encounters straight-curved-straight or curved-straight-curved connections. For very gradual bends it is merely necessary to account for the forward coupling at each junction since any reflections are negligible. Sharp bends, on the other hand, require one to account for multiple reflections; this appears to be most effectively handled by the scattering matrix approach.

VI. ACKNOWLEDGMENT

The author wishes to express his appreciation to Dr. J. Alan Cochran and Mr. C. M. Nagel who actively participated in and constructively contributed to many phases of this work and to Dr. C. P. Wu who, in many helpful discussions, so generously shared with us his knowledge and experience in the numerical solution of problems of this type. Thanks are also expressed to Miss E. J. Murphy who programmed a good deal of the numerical work associated with this problem.

REFERENCES

1. Cochran, J. Alan, and Pecina, Robert G., "Mode Propagation in Continuously Curved Waveguides," *Radio Sci.*, 1 (new series), No. 6 (June 1966), pp. 679-695.
2. Rice, S. O., "Reflections from Circular Bends in Rectangular Wave Guides—Matrix Theory," *B.S.T.J.*, 27, No. 2 (April 1948), pp. 305-349.
3. Jouguet, M., "Les effets de la courbure et des discontinuités de courbure sur la propagation des ondes dans les guides à section rectangulaire," *Câbles et Transmission*, 1, No. 1 (April 1947), pp. 39-60.
4. Cochran, J. Alan, Nagel, C. M., and Alsberg, P. A., unpublished work.
5. Harrington, R. F., *Time Harmonic Electromagnetic Fields*, New York: McGraw-Hill, 1961.
6. Cochran, J. Alan, "Remarks on the Zeros of Cross-Product Bessel Functions," *J. Soc. Ind. Appl. Math.*, 12, No. 3 (September 1964), pp. 580-587.
7. Harrington, R. F., "Matrix Methods for Field Problems," *Proc. IEEE*, 55, No. 2 (February 1967), pp. 136-149.
8. Kislyuk, M. Zh., "Waveguide Bend of Rectangular Cross-Section," *Radio Eng.*, 16, No. 4 (April 1961), pp. 1-8.
9. Olver, F. W. J., "The Asymptotic Expansion of Bessel Functions of Large Order," *Trans. Royal Soc. London*, 247, Series A, (1954), pp. 328-368.
10. Abramowitz, M., and Stegun, I., *Handbook of Mathematical Functions*, New York: Dover Publications, 1965.
11. Amitay, N., and Galindo, V., "On Energy Conservation and the Method of Moments in Waveguide Discontinuity and Scattering Problems," 1969 United States Nat. Committee of the Int. Sci. Radio Union Spring Meeting, April 21-24, 1969, Washington, D. C.
12. Cole, W. J., Nagelberg, E. R., and Nagel, C. M., "Iterative Solution of Waveguide Discontinuity Problems," *B.S.T.J.*, XLVI, No. 3 (March 1966), pp. 649-672.